Nordic Hydrology, 26, 1995, 331-358

Spring Circulation Associated with the Thermal Bar in Large Temperate Lakes

Joakim Malm
Department of Water Resources Engineering,
Lund University, Sweden

The overall circulation pattern in spring is rather specific as density-induced currents may be of significance. The density-driven circulation perpendicular to the shore can be described as consisting of two circulation cells, with a zone of convergence, referred to as thermal bar, in between. The thermal bar, which coincides with the 4°C isotherm (the temperature of maximum density), inhibits horizontal water exchange, implying its practical importance. In this paper, a hydrodynamic numerical model is used to study the relative influence of wind- and density-driven currents in a large temperate lake during spring.

The study shows that the general density-driven circulation is strongly dependent on the bottom topography, with a more pronounced circulation and considerable descending motions in the thermal bar zone in lakes with steep sloping bottoms. In shallow lakes, the wind-driven circulation dominates, and the effect of density-induced currents is marginal, except at locations with a drastic change in bottom depth.

Introduction

The temperature pattern and its development during spring in large temperate lakes have a special character, due to the fact that freshwater has its highest density at 4°C. Just after the ice cover has vanished, the temperature in the lake is almost homogeneous and below 4°C. As the spring heating proceeds, convective mixing leads to isothermal conditions with depth and a faster increase in temperature in the shallow near-shore regions than in the deeper parts of the lake. When the temperature reach-

es and exceeds 4°C at the shore, a stable temperature stratification develops. Between this region and the main part of the lake, where the water is convectively mixed and with constant temperatures throughout a vertical, there is a zone of descending water with temperature of maximum density. This zone, named thermal bar, is of practical importance as it has an inhibiting effect on the horizontal water exchange. In the course of warming, the thermal bar moves towards the deep parts of the lake, until it finally vanishes and the temperature stratification with horizonal isotherms characteristic for the summer period sets in. In large lakes like the Great Lakes in North America, Lake Ladoga, Lake Onega, and Lake Vänern in Europe the time of thermal bar existence is about one to a couple of months.

The interest for the spring thermal regime and its associated circulation in large temperate lakes was initiated by the studies of Tikhomirov (1959; 1963). He tried to explain the circulation associated with the thermal bar, as consisting of two circulation cells, one at each side of the bar. The surface current in both the stably stratified near-shore region and in the convectively mixed deep parts of the lake, was suggested to be directed towards a zone of convergence with extensive vertical water motions, the thermal bar. The return current along the bottom, should then by continuity reasons be directed away from the bar. Indications that supported this theory concerning the surface currents were visible bands of foam and floating objects at the water surface located along the 4°C isotherm. Rodgers (1965; 1966), who made the first detailed studies of the spring thermal regime in the Great Lakes in North America confirmed Tikhomirov's thoughts of the thermal bar being a zone of convergence by performing drogue measurements and by, as Tikhomirov did, finding a similar visual band above the 4°C isotherm, consisting of dead fish, algae, and debris. He also found indications of the two-cell circulation pattern from studies of the horizontal transport of heat during spring (Rodgers, 1966; 1968; 1971). This circulation was, however, suggested to be secondary, superimposed on a primary density-induced circulation along the isotherms that would be at least one order of magnitude greater.

Only a few field investigations of the spring circulation associated with the thermal bar have been made. They mostly show an influence of earlier or present wind conditions (see for instance Malm *et al.*, 1991; 1992) on the circulation pattern. One may therefore assume that the influence on the circulation by the horizontal density gradients is comparatively weak. However, the density-driven circulation exists throughout the spring period.

Several models, both analytical and numerical, describing the density-induced circulation have been developed. The first analytical model by Elliot (1971), did not account for the earth rotation. The obtained circulation was similar to the one outlined by Tikhomirov, with two circulation cells on each side of the thermal bar. The results were also compared with the observed velocity fields in a small laboratory tank, and good agreement was found.

Analytical models of the density-driven circulation in Great Lakes, including the

Coriolis terms, have been derived by Huang (1971; 1972) and Brooks and Lick (1972). The simulation results from these models agreed well with the thoughts of Rodgers, with a primary circulation parallel to the isotherms that is cyclonic (anticlockwise) between the shore and the thermal bar and anticyclonic (clockwise) in the central convectively mixed region of the lake. The simulated secondary circulation was principally the same as described by Tikhomirov. Estimates of the maximum long-shore and cross-shore velocities was about 10^{-1} m sec^{-1} and 10^{-2} m sec^{-1}, respectively. Partly based on these calculations, Huang (1972) stressed the inhibiting effect of the thermal bar on the horizontal water exchange.

A two-dimensional numerical model to study the thermally-driven circulation during spring was made by Bennet (1971). The calculated thermally-driven circulation pattern was qualitatively similar to the ones derived by Huang (1971; 1972) and Brooks and Lick (1972). However, the magnitude of the current velocities was less with a maximum longshore current of 2-3 cm sec^{-1}. Benn*et al*so calculated the horizontal heat transport perpendicular to the shore. The results are consistent with the observed heat content changes by Rodgers (1966), which indicates that the calculated circulation pattern is realistic. Scavia and Bennet (1980) calculated the current structure during spring in Lake Ontario using an observed wind field. They concluded that the flow is dominated by wind, but that the thermally-driven circulation is equally important due to its persistence.

Csanady (1971; 1972; 1974) investigated the flow pattern in Lake Ontario during the time of thermal bar existence in connection with some events with high wind speeds. He stated that a spring thermocline coinciding with the 6 or 7°C isotherm separates the warm coastal waters from the cold main lake mass (Csanady 1974). This inclined surface can either take the shape of a wedge or a lens, depending on the direction of flow (Csanady 1972). A wedge-shaped thermocline is associated with a shore parallel current directed to the right seen from the shore, and a lens-shaped thermocline is associated with a shore-parallel current directed to the left seen from the shore. In connection to high wind events during spring the current characteristics of the shore zone are quite different from those in the offshore zone. The near-shore zone is dominated by relatively persistent bands of currents with typical velocities of the order of 20 cm sec^{-1}, while the offshore region experiences relatively small current velocities of the order of 5 cm sec^{-1} or less (Csanady 1972). The high wind events are, however, seldom strong enough to break down the stratification in the warm zone (Csanady 1974).

The magnitude of the sinking velocities in the thermal bar zone is important for the circulation. Carmack and Farmer (1982) estimated the vertical velocity to be of the order of 10^{-2} cm sec^{-1} during autumn in Babine Lake, and the mathematical models made by Huang (1972), Brooks and Lick (1972), and Bowman and Okubo (1978) showed that the vertical velocities in the spring thermal bar zone should be of the order of 10^{-2}, 10^{-1} and 10^{-2} cm sec^{-1}, respectively. The vertical velocities in the thermal bar zone are thus too small to be detected by current meters in field.

The objective of this paper is to qualitatively describe the effect of wind on the circulation pattern during spring in a large temperate lake and to what extent the thermal bar functions as a barrier for horizontal water exchange. According to Scavia and Bennet (1980), the wind circulation tends to drive a one-cell pattern over a cross-section of a lake as opposed to the density-driven circulation. Therefore, in this study winds of different magnitude and direction are imposed to an initially thermally-driven double-cell current system with an established thermal bar, and the transition towards a one-cell circulation pattern is investigated. First, however, the magnitude of the general thermally-driven circulation in a cross-section of a lake is calculated for different hypothetical situations to get background information on their structure and importance.

In the study a two-dimensional numerical hydrodynamic model is used because the objectives of the study are of a principle character and not to describe details or three-dimensional effects.

Description of the Hydrodynamic Model used

A two-dimensional numerical hydrodynamic model is used, in which a cross-section of a lake with an arbitrary bottom topography perpendicular to the shore, but homogeneous along the shore is considered, see Fig. 1. All gradients of temperature and velocities perpendicular to the section, $(\partial/\partial x)$, are assumed to be zero, but a longshore pressure gradient, $(\partial p/\partial x)$, dependent on time, is accounted for in order for the total volume flow perpendicular to the cross-section to be zero (see Eq. (5) below). To model the thermo-hydrodynamics for this cross-section, the following set of equations is used

$$\frac{\partial u}{\partial t} + v\frac{\partial u}{\partial y} + w\frac{\partial u}{\partial z} = fv - \frac{1}{\rho_0}\frac{\partial p'}{\partial x} + \frac{\partial}{\partial y}\left(A_h\frac{\partial u}{\partial y}\right) + \frac{\partial}{\partial z}\left(A_v\frac{\partial u}{\partial z}\right) \tag{1}$$

$$\frac{\partial v}{\partial t} + v\frac{\partial v}{\partial y} + w\frac{\partial v}{\partial z} = -fu - \frac{1}{\rho_0}\frac{\partial p'}{\partial y} + \frac{\partial}{\partial y}\left(A_h\frac{\partial v}{\partial y}\right) + \frac{\partial}{\partial z}\left(A_v\frac{\partial v}{\partial z}\right) \tag{2}$$

$$\frac{\partial w}{\partial t} + v\frac{\partial w}{\partial y} + w\frac{\partial w}{\partial z} \equiv -\frac{1}{\rho_0}\frac{\partial p'}{\partial z} - \rho' g + \frac{\partial}{\partial y}\left(A_h\frac{\partial w}{\partial y}\right) + \frac{\partial}{\partial z}\left(A_v\frac{\partial w}{\partial z}\right) \tag{3}$$

$$\frac{\partial v}{\partial y} + \frac{\partial w}{\partial z} \equiv 0 \tag{4}$$

$$\int_0^L \int_{-D(y)}^0 u\, dz\, dy = 0 \tag{5}$$

$$\frac{\partial T}{\partial t} + v\frac{\partial T}{\partial y} + w\frac{\partial T}{\partial z} = K_h\frac{\partial^2 T}{\partial y^2} + \frac{\partial}{\partial z}\left(K_v\frac{\partial T}{\partial z}\right) \tag{6}$$

$$\rho = \rho_m\left(1 - \frac{1}{2}\alpha(T-T_m)^2\right) \tag{7}$$

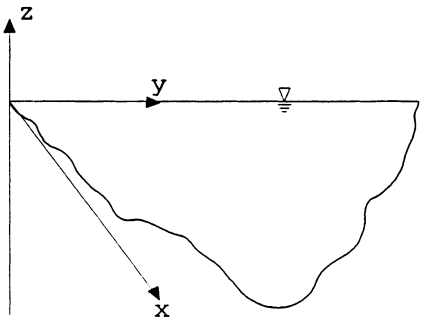

Fig. 1. A cross-section of a lake with an arbitrary bottom topography perpendicular to the shore (y-axis), but with constant depths along the shore (x-axis). The velocity and temperature fields are also considered as homogeneous along the x-axis.

Eqs. (1), (2), and (3) are the hydrodynamic differential equations of motion (where the Boussinesq approximation is used) for the longshore (x-direction), cross-shore (y-direction) and vertical (z-direction) velocity components. Eq. (4) is the continuity equation for the cross-section, Eq. (5) is the requirement of a total zero net flow perpendicular to the section, and Eqs. (6) and (7) are the heat transfer equation (divided by density and specific heat of water) and the quadratic form of the state equation for freshwater, respectively. The introduced variables and parameters are:

u, v, w	=	average current velocity components in x, y, and z direction
t	–	time
f	=	Coriolis parameter (set to 1×10^{-4} sec^{-1} as a typical value in the northern hemisphere)
p'	–	deviation from the pressure at the state of rest
ρ_0	=	reference density for freshwater
ρ'	=	deviation from the reference density
g	=	gravity acceleration (=9.81 m sec^{-2})
A_h and A_v	=	horizontal and vertical eddy viscosities
L	=	length of the cross-section
$D(y)$	=	bottom depth at a distance y along the cross-section
T	–	water temperature
K_h and K_v	=	horizontal and vertical eddy conductivities
ρ	–	water density
ρ_m	=	maximum freshwater density (=1000 kg m^{-3})
a	=	constant in the quadratic state equation for freshwater
	=	(=1.65 × 10-5°C^{-2}, from Carmack and Farmer 1982)
T_m	=	temperature of maximum density (=4.0°C)

The following boundary conditions are used at the solid bottom boundary, z=-$D(y)$,

$$u = v = w = 0 \tag{8}$$

$$Q_b = 0 \tag{9}$$

and at the free surface

$$\rho A_v \frac{\partial u}{\partial z} \equiv \tau_x, \quad \rho A_v \frac{\partial v}{\partial z} = \tau_y \tag{10}$$

$$\tau \equiv \sqrt{\tau_x^2 + \tau_y^2} \equiv C_D \rho_a W^2 \tag{11}$$

$$w = 0 \tag{12}$$

$$-\rho_0 c_p K_v \frac{\partial T}{\partial z} = Q_s \tag{13}$$

where the rigid lid approximation, Eq. (12), has been used. (In the rigid lid approximation, the displacement of the free surface is neglected, and the surface gravity waves are filtered out. However, the pressure under the lid can be related to the free surface displacement, Bennet (1974)). In these expressions the following additional variables and parameters have been introduced:

Q_b – bottom heat flux
Q_s – heat flux at the water surface
c_p – specific heat of water (set to 4.19×103 J kg^{-1}·°C-1)
τ – total wind stress at the water surface
τ_x, τ_y – wind stress components in x- and y-direction, respectively
C_D – drag coefficient
ρ_a – density of air (taken as 1.25 kg m^{-3})
W – wind velocity at 10 m above the water surface

C_D is set to 1.3×10^{-3}, a value taken from a review by Svensson (1978).

The methodology used to solve the system of equations for the hydrodynamic model is similar to the one used in the numerical model PHOENICS (*e.g.*, Spalding 1992). The governing equations are discretisized using the control volume formulation with a upwind scheme for the convective terms. The SIMPLE algorithm (see Patankar (1980) for a detailed description of SIMPLE type schemes) applied on a staggered mesh is then used for calculation of the flow (temperature) field. A uniform grid with the size 80 (horizontal) * 20 (vertical) was used in the calculations below. The time steps used were 1800, 900, and 100 seconds for the three lake sections considered below (section A, B, and C, respectively).

The model is similar to the one used by Bennet (1971) to numerically predict the general thermally-driven spring circulation. There is, however, one main difference. The thermal bar is a zone with substantial vertical water transport according to the suggestions by Tikhomirov (1963) and Rodgers (1965). Therefore, for a correct description of the circulation in this zone, the vertical momentum equation is used instead of the hydrostatic equation.

Determination of Turbulent Exchange Coefficients

As this study of the spring circulation in large lakes is of a qualitative nature, no effort will be made to model turbulence characteristics. Instead, the turbulent exchange coefficients (A_h, A_v, K_h, and K_v) are crudely expressed as constants. The influence of buoyancy effects in the stably stratified region of the lake will be considered by the use of simple expressions. This is important since the turbulent transport of heat and momentum may be considerably reduced due to the stable stratification. This was not considered in the theoretical study of the thermally driven currents in temperate lakes during spring by Bennet (1971). Reasonable values on the exchange coefficients will be determined below on basis of estimates from simple formulas and models.

The horizontal eddy viscosity and conductivity coefficients (assumed to be equal) are estimated using the four-thirds law

$$A_h = K_h = \alpha L^{4/3} \tag{14}$$

where α is a dimensional diffusion parameter set to $1 \times 10\text{-}2$ cm$^{2/3}$ sec^{-1} (*cf.*, Harleman and Stolzenbach, 1972) and L is a length scale for the horizontal turbulent motion. Because the present study is focussed on the thermal bar, it seems appropriate to choose the bar zone width as the length scale, L. The width of the thermal bar zone is, however, not easily defined. It can be of the same order as the bottom depth, as suggested by Zilitinkevich *et al.* (1992), or as the width of the region with large temperature gradients, which can be of the order of several hundreds of metres. Here, the grid step Δy, chosen to be as close to the magnitude of the bar zone width as possible, is used as the length scale L.

Rough estimates of the average vertical exchange coefficients have to be made for three different conditions. 1) For the density-driven circulation in a neutrally stratified near-shore region, the eddy viscosity can be estimated using Prandtl's free-shear-layer model for a plane mixing layer (Rodi 1980),

$$A_{v0} \equiv 10^{-2} \delta U \tag{15}$$

where δ is the layer width (set equal to the depth, D), and U is a velocity scale. 2) In the unstably stratified and convectively mixed »deep-water« region, the eddy viscosity can be determined from the following depth averaged expression, proposed by Malm and Zilitinkevich (1994)

$$A_{v0} \equiv 0.06 \left(\frac{g \alpha (T - T_m) Q_s}{\rho_0 c_p} \right)^{1/3} D^{4/3} \tag{16}$$

3) In the presence of a wind stress, the following expression for the depth-averaged eddy viscosity in a neutrally stratified environment seems appropriate (Malm and Zilitinkevich 1994),

$$A_{v0} = 0.04 u_* D \tag{17}$$

where u^* is the friction velocity ($=(\tau/\rho)^{1/2}$).

Using a depth scale of 30 m (typical for the model calculations below), and the following typical values, $U = 0.05$ m sec^{-1} (according to a study of the spring dynamics in Lake Ontario by Csanady (1972), the maximum current velocity during calm conditions was usually 5 cm sec^{-1} or less), T = 2.5°C, $Q_s = 200$ W m^{-2}, and $u^* = 0.01$ m sec^{-1} (corresponding to a considerable windstress of 8 m sec^{-1}), the magnitude of the vertical eddy viscosity is approximately 10^{-2} m^2 sec^{-1} for all three cases. The vertical eddy conductivity is assumed to correspond to the eddy viscosity, except in the convectively mixed region, where the effective vertical eddy conductivity is about 10 times larger than the effective vertical eddy viscosity (see, *e.g.*, the collection of experimental data on the turbulent Prandtl number in unstable stratification in Zilitinkevich 1970).

To account for the buoyancy effects on the vertical turbulent transport of heat and momentum in the near-shore region, the following empirical formulas, proposed by Munk and Anderson (1948), for A_v and K_v are used

$$A_v = A_{v0}(1+10R_i)^{-0.5}, \quad K_v = K_{v0}(1+3.33R_i)^{-1.5} \tag{18}$$

where A_{v0} and K_{v0} are the eddy viscosity and eddy conductivity for neutrally stratified conditions, respectively. R_i is defined by

$$R_i \equiv -\frac{g}{\rho}\frac{\partial\rho/\partial z}{(\partial u/\partial z)^2} \tag{19}$$

From these separate estimates, it is now possible to define appropriate values on the exchange coefficients to be used in the hydrodynamic model. These are given in Table 1.

Table 1 – The turbulent exchange coefficients used in the hydrodynamic model as a function of Richardson number, R_i

	A_h (m^2 sec^{-1})	K_h (m^2 sec^{-1})	A_v (m^2 sec^{-1})	K_v (m^2 sec^{-1})
Ri≥0	$4.6\times10^{-4}(\Delta y)^{4/3}$	$4.6\times10^{-4}(\Delta y)^{4/3}$	$1\times10^{-2}(1+10\times Ri)^{-0.5}$	$1\times10^{-2}(1+3.33\times Ri)^{-1.5}$
Ri<0	$4.6\times10^{-4}(\Delta y)^{4/3}$	$4.6\times10^{-4}(\Delta y)^{4/3}$	1×10^{-2}	1×10^{-1}

General Density-driven Circulation During Spring

The objective of this section is to model and analyze the temperature structure and the corresponding thermally-driven circulation in a cross-section of different idealized lakes, when the thermal bar is fully developed. Some of the calculated temperature and current structures below will also be used as initial conditions in the next

section, when the effect of a wind stress on the spring circulation in large temperate lakes is investigated. A qualitative picture of the temperature structure and circulation pattern in a large temperate lake during spring in the absence of wind was obtained, as mentioned above, by Bennet (1971) from results of a two-dimensional numerical model. The calculated temperature distribution was also shown to be in qualitatively good agreement with some observations from Lake Ontario. In the study, however, he implicitly considered vertical wind mixing by the use of a constant turbulent exchange coefficient. In the present study, situations when the temperature structure both has and has not been subject to considerable vertical heat mixing (by the use of a stratification dependent and a constant turbulent exchange coefficient, respectively) are investigated. Also the influence of the bottom topography on the temperature and circulation structure is studied. A non-uniform bottom depth is the primary cause for the horizontal temperature gradients.

The studied situations are of an artificial nature as the main aim is to investigate the bulk spring circulation. The calculations by the hydrodynamic model described above are performed for three different cross-sections. In Europe's largest freshwater lake, Lake Ladoga, the average bottom slope ranges from 1×10^{-3} in the southern part to 1×10^{-2} in the northern areas. Typical average bottom slopes for other large freshwater lakes in Europe, like Lake Onega in Russia and Lake Vänern in Sweden, and the Great Lakes in North America are also within these ranges. These limits are the chosen uniform bottom slopes for two of the model sections, named A (slope = 10^{-2}) and B (slope $\equiv 10^{-3}$), shown in Figs. 2 and 3 below. The third section, named C (shown in Fig. 6), is intended to illustrate a more special and local situation with a sudden change in bottom depth. This section is idealized to consist of one shallow and one deep water region, both with constant bottom depths, and a rapid change in bottom depth in between (with a constant slope set to 8×10^{-2}). The interest in studying such a specific situation is that the thermal bar ought to be almost stationary at the position of the drastic change in bottom depth. As the bottom depth is constant before and after the jump in bottom depth, it seems likely that the circulation in the thermal bar zone will be more pronounced compared to the general circulation in the section, and perhaps also a cause for it.

The surface heat flux, Q_s, which is the source for the density-driven motion, will be taken as constant in time and space with a value of 210 W m^{-2} (typical values for the surface heat flux in spring are for Lake Ladoga 200-250 W m^{-2}, see Malm *et al.* 1991; 1992, and about 210 W m^{-2} for Lake Ontario, see Rodgers 1968; Rodgers and Sato 1970). To introduce an external heat flux only as a boundary condition at the surface, however, is not correct at least not during periods of limited vertical mixing. A large portion of the incoming heat comes from direct solar radiation that penetrates into the water body. The surface heat flux is introduced as a heat source in the upper layer of the lake, and is distributed in accordance with the penetration of solar radiation into the water. The penetration of the solar radiation into the water mass can be estimated as (*e.g.*, Henderson-Sellers 1984)

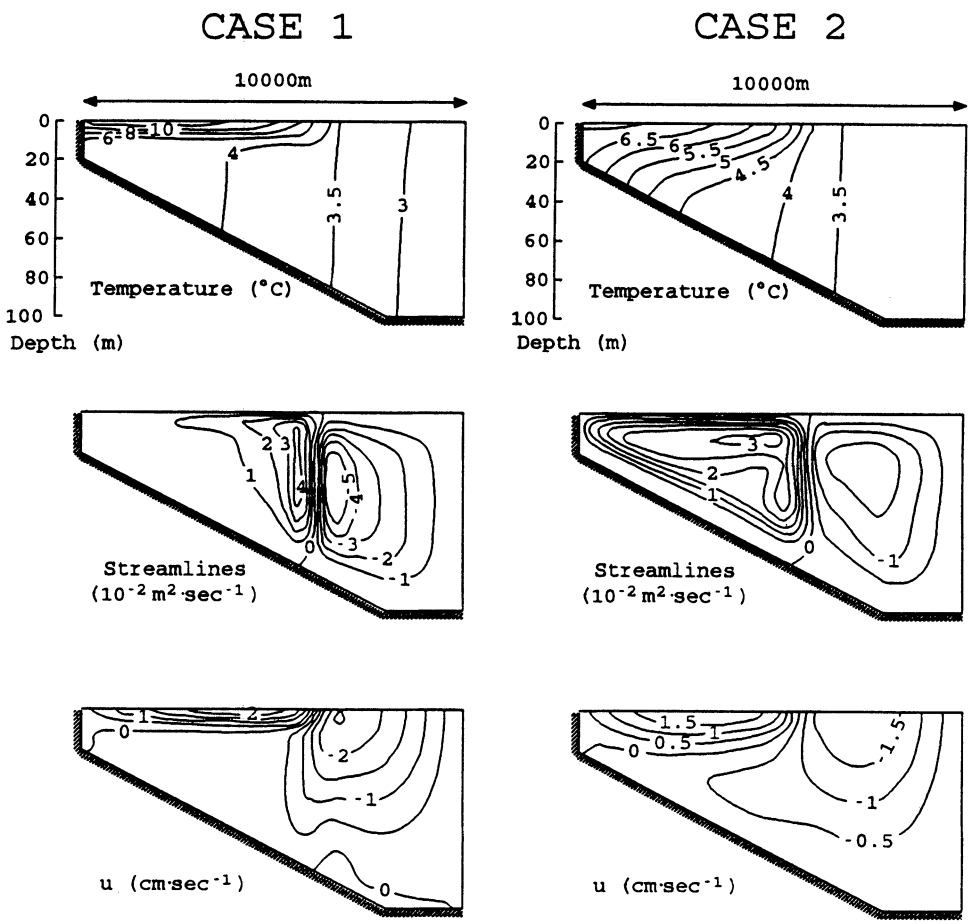

Fig. 2. Obtained temperature distributions, streamfunctions, and long-shore velocity distributions for cases 1 and 2 (section A, with the bottom slope 10^{-2}) when only density-driven currents were considered. Only half of the cross-section is shown as the center is a symmetry line.

$$\phi(z) = (1-\gamma)\phi_0 \exp(-\eta z) \tag{20}$$

where $\phi(z)$ is the total shortwave radiation reaching the depth z, ϕ_0 is the shortwave radiation at the water surface, η is the extinction coefficient and γ (fraction of the radiation that is absorbed in the surface layer) is expressed by

$$\gamma = 0.265 \ln(\eta) + 0.614 \tag{21}$$

The extinction coefficient, η, is on average approximately 0.29 m^{-1} in the Great Lakes in North America and 0.34 m^{-1} in Lake Ladoga (Petrova and Terzhevik 1992). In the following the extinction coefficient is set to 0.3 m^{-1}.

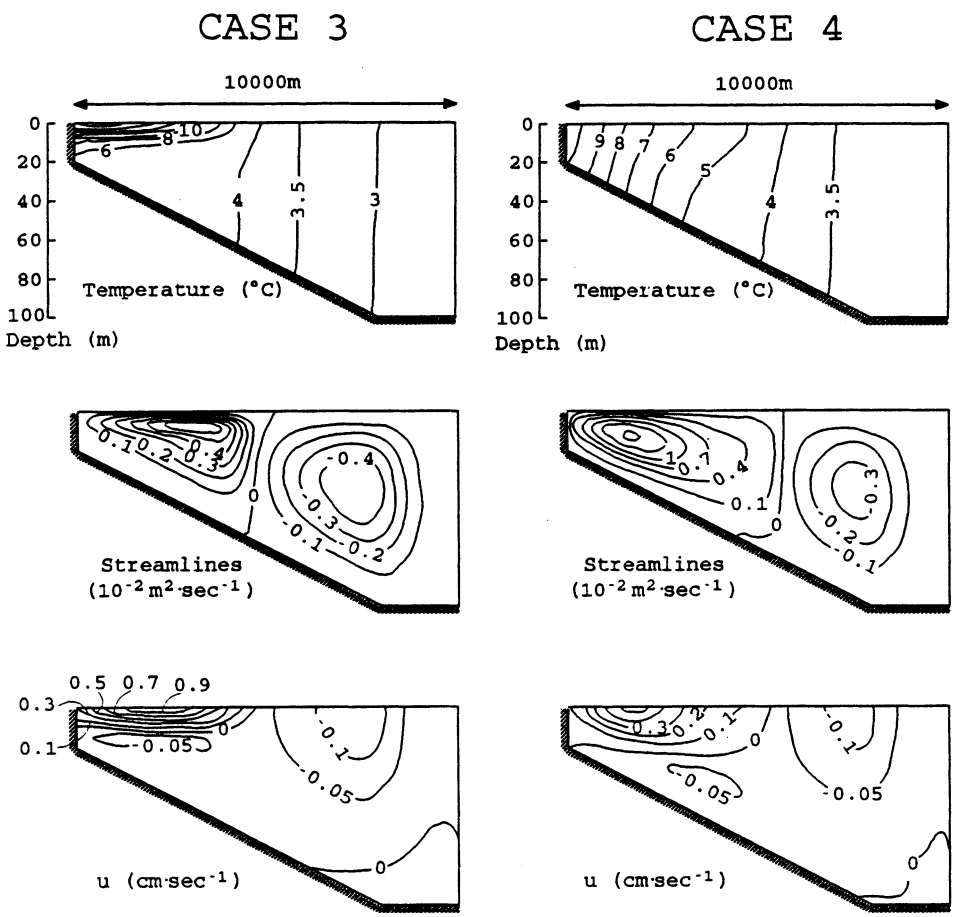

Fig. 3. Obtained temperature distributions, streamfunctions, and long-shore velocity distributions for cases 3 and 4 (section B, with the bottom slope 10^{-3}) when only density-driven currents were considered. Only half of the cross-section is shown as the center is a symmetry line.

The initial temperature in the lake at the onset of the spring circulation period is taken as constant in space with a value of 1°C (typical reference values from Lake Ladoga and Lake Ontario are 0.5°C and 2.0°C, see Malm *et al.*, 1994; Rodgers 1966). The initial current velocities are set to 0 m sec^{-1}.

The constant vertical turbulent exchange coefficients, used in the calculations where the vertical mixing is emphasized, are set to different values in the stably stratified and convectively mixed regions. In the latter the values from above, A_v=1 × 10^{-2} m^2 sec^{-1} and K_v=1 × 10^{-1} m^2 sec^{-1} are used. In the near-shore region the values based on neutral stratification are reduced somewhat to account for the tempera-

ture stratification, by crudely setting the Richardson number to 2. Thus the following constant values on the exchange coefficient are used $A_v=2.2 \times 10^{-3}$ m^2 sec^{-1} and $K_v=4.7 \times 10^{-4}$ m^2 sec^{-1} (which can be compared to the values $A_v=4.5 \times 10^{-3}$ m^2 sec^{-1} and $K_v=7.5 \times 10^{-4}$ m^2 sec^{-1} used by Bennet (1971) and $A_v=3.0 \times 10^{-3}$ m^2 sec^{-1} and $K_v=3.0 \times 10^{-3}$ m^2 sec^{-1} used by Huang, 1971, for similar studies). The parameters used in the model calculations for the different sections and cases are summarized in Table 2.

Table 2 – Parameters used in the numerical calculations for the three cross-sections. T_0 is the initial temperature in the lake; t_{tot} is the total simulated time from the initial conditions; Δt, Δy and Δz are the time step, horizontal and vertical grid steps, respectively

Section	A		B		C
Case	1	2	3	4	5
Q_s (W m^{-2})	210	210	210	210	210
T_0 (°C)	1	1	1	1	1
A_h (m^2 sec^{-1})	0.73	0.73	6.25	6.25	0.085
K_h (m^2 sec^{-1})	0.73	0.73	6.25	6.25	0.085
A_v (m^2 sec^{-1})	[1]$1\times10^{-2}(1+10\,R_i)^{-0.5}$, [2]$1\times10^{-2}$	[1]2.2×10^{-3}, [2]1×10^{-2}	[1]$1\times10^{-2}(1+10\,R_i)^{-0.5}$, [2]$1\times10^{-2}$	[1]2.2×10^{-3}, [2]1×10^{-2}	[1]2.2×10^{-3}, [2]1×10^{-2}
K_v (m^2 sec^{-1})	[1]$1\times10^{-2}(1+3.33\,R_i)^{-1.5}$, [2]$1\times10^{-1}$	[1]4.7×10^{-4}, [2]1×10^{-1}	[1]$1\times10^{-2}(1+3.33\,R_i)^{-1.5}$, [2]$1\times10^{-1}$	[1]4.7×10^{-4}, [2]1×10^{-1}	[1]4.7×10^{-4} [2]1×10^{-1}
t_{tot} (days)	42	42	22	22	21
Δt (sec)	1,800	1,800	900	900	100
Δy (m)	250	250	1,250	1,250	50
Δz (m)	5	5	2.5	2.5	2

[1]$R_i \geq 0$, [2]$R_i < 0$

Results – Sections A and B

The results of the calculations of the temperature structures and associated density-driven currents for the sections with constant bottom slopes are shown in Figs. 2 and 3, and summarized in Table 3. (The time needed to establish the thermal bar at the shore from the initially temperature homogeneous conditions ($T_0 \equiv 1$°C) was approximately two weeks for section A and one week for section B). The temperature distributions show different pictures in the »warm« near-shore region, when the vertical exchange coefficient is a function of Richardson number and when it is constant. In the former case, the limited vertical heat exchange leads to a narrow wedge of warm water at the surface, extending from the shore to the thermal bar, where the isotherms are almost horizontal. Below this wedge the water is close to the temperature of maximum density, 4°C. This situation is qualitatively very similar to what has been observed in large temperate lakes during periods of calm weather. One such example from Lake Ontario is shown in Fig. 4.

Table 3 – Summary of results from calculations of the temperature structures and associated density-driven circulation for the sections with constant bottom slopes (see also Figs. 2 and 3)

		Section A (bottom slope = 10^{-2})		Section B (bottom slope = 10^{-3})	
		Case 1 (A_z, K_z = f(Ri))	Case 2 (A_z, K_z = constant)	Case 3 (A_z, K_z = f(Ri))	Case 4 (A_z, K_z = constant)
Temperature Characteristirs	Near-shore zone	Narrow wedge of warm water at the surface with strong vertical temperature gradients. Almost isothermal region (temp. close to 4°C) between this wedge and bottom.	Inclined isotherms and rather homogeneous temperature gradients, (except in vicinity of the 4°C isotherm, close to bottom, where gradients are weaker).	Narrow wedge of warm water at the surface with strong vertical temperature gradients. Almost isothermal region (temp.close to 4°C) between this wedge and bottom.	Well-mixed conditions and almost vertical isotherms, except in vicinity of the 4°C isotherm, where isotherms are slightly inclined.
	Offshore zone	Vertically well-mixed with almost depth-constant temperatures.	Vertically well-mixed with almost depth-constant temperatures.	Vertically well-mixed with almost depth-constant temperatures.	Vertically well-mixed with almost depth-constant temperatures.
Circulation Characteristics	Near-shore zone	Closed circulation cell. Surface current towards the bar and bottom current away from the bar. Main horizontal water motions at the narrow wedge of warm water. $u_{max} \approx 2$ cm sec^{-1}, $v_{max} \sim 0.7$ cm sec^{-1}.	Closed circulation cell. Surface current towards the bar and bottom current away from the bar. Pronounced currents in the entire region, with largest velocities at the surface umax~2 cm sec^{-1}, $v_{max} \sim 0.5$ cm sec^{-1}.	Closed circulation cell. Surface current towards the bar and bottom current away from the bar. Main horizontal water motions at the narrow wedge of warm water. $u_{max} \sim 1$ cm sec^{-1}, $v_{max} \sim 0.3$ cm sec^{-1}.	Closed circulation cell. Surface current towards the bar and bottom current away from the bar. Circulation covers entire region, with largest velocities at the surface. $u_{max} \sim 0.4$ cm sec^{-1}, $v_{max} \sim 0.35$ cm sec^{-1}.
	Thermal bar zone	Convergence zone, with strong descending motions. $w_{max} \sim -0.5$ mm sec^{-1}.	Convergence zone, with pronounced descending motions. $w_{max} \sim -0.1$ mm sec^{-1}.	Convergence zone, without pronounced descending motions. $w_{max} \sim < -0.01$ mm sec^{-1}.	Convergence zone, without pronounced descending motions. $w_{max} \sim < -0.01$ mm sec^{-1}.
	Offshore zone	Closed circulation cell. Surface current towards the bar and bottom current away from the bar. Pronounced currents in entire region with highest velocities at the surface in vicinity of the 4°C isoterm. $u_{max} \approx -2$ cm sec^{-1}, $v_{max} \sim -0.5$ cm sec^{-1}.	Closed circulation cell. Surface current towards the bar and bottom current away from the bar. Pronounced currents in entire region with highest velocities at the surface. $u_{max} \sim -2$ cm sec^{-1}, $v_{max} \approx -0.2$ cm sec^{-1}.	Closed circulation cell. Surface current towards the bar and bottom current away from the bar. Weak currents in entire region with highest velocities at the surface. $u_{max} \sim -0.1$ cm sec^{-1}, $v_{max} \sim -0.05$ cm sec^{-1}.	Closed circulation cell. Surface current towards the bar and bottom current away from the bar. Weak currents in entire region with highest velocities at the surface. $u_{max} \sim -0.15$ cm sec^{-1}, $v_{max} \sim -0.05$ cm sec^{-1}.

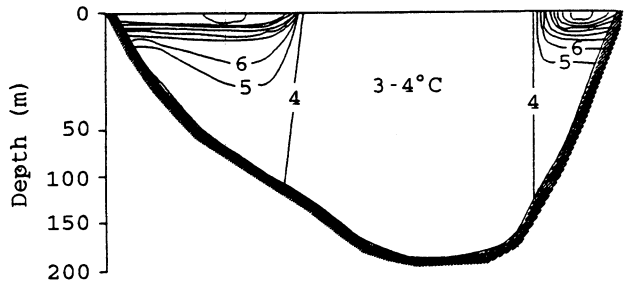

Fig. 4. Observed temperature distribution in Lake Ontario during 7-10 June, 1965 (after Rodgers 1966). The distance from shore to shore is approximately 65 km.

In the presence of a wind stress, the vertical heat mixing is more extensive on the shore-side of the 4°C isotherm, than described by cases 1 and 3. This was artificially considered by the use of constant turbulent exchange coefficients in cases 2 and 4. In these latter cases the temperature distributions in the near-shore region show also much more inclined isotherms and a larger volume of water with a temperature well above 4°C. Also these pictures are in qualitative accordance with what has been observed during periods of windy conditions. An example from Lake Ladoga that can be compared with the temperature distribution for the case with a bottom slope of 10^{-3} is shown in Fig. 5.

For all simulated situations the temperature is approximately depth constant offshore the 4°C isotherm, because of strong vertical mixing by convection, which is in good agreement with field observations. There is no essential qualitative difference in the temperature distributions due to different bottom slopes, except that vertical mixing is a little higher in the more shallow and less sloping section. There are two circulation cells, with a convergence zone, *i.e.*, thermal bar zone, approximately where the 4°C isotherm intersects the water surface. The surface current is directed

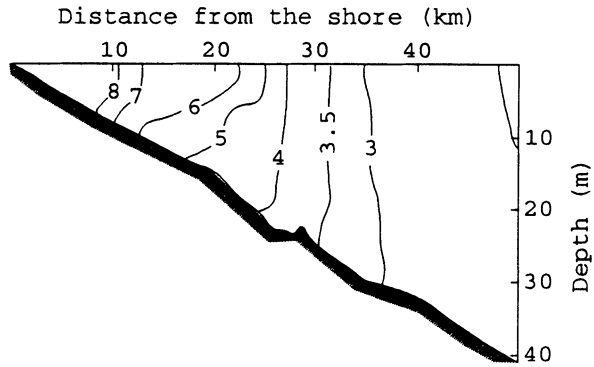

Fig. 5. Observed temperature distribution in Lake Ladoga, 26 May, 1991 (after Malm *et al.*, 1993).

towards the bar, both in the near-shore stably stratified region and in the convectively mixed region, and the bottom current is directed away from the bar. The main water motions are located near the water surface in the near-shore region. The thermal bar as a zone of extensive vertical water movement is more pronounced when the vertical exchange coefficients on the shore-side of the bar are functions of Richardsons number. The velocity field becomes more homogeneous when the vertical exchange coefficients are constants. The magnitude of the currents are larger when the bottom slope is steeper, due to the larger horizontal temperature gradients. The thermal bar is also much more pronounced when the bottom slope is steep.

The pronounced thermal bar at steep sloping bottoms can be explained by comparing the long-section velocities in the near-shore region with the speed of the thermal bar. The average thermal bar progression rates (determined as the distance passed by the bar divided by the time difference from its initiation to the end of the calculations), are approximately 0.2 cm sec^{-1} for section A and 2.0 cm sec^{-1} for section B. The horizontal velocities at the water surface along the section are about 0.5 cm sec^{-1} for section A and about 0.3 cm sec^{-1} for section B. Thus, the thermal bar progresses faster than heat is advected along the water surface in the near-shore region when the bottom slope is 10^{-3} (section B), which indicates that the conditions for mixing of warm and cold water at the thermal bar are minimized, and so are the descending motions. When the bottom slope is 10^{-2} (section A) the situation is the opposite; the conditions are favorable for extensive vertical water movements in the thermal bar zone.

Results – Section C

The computed temperature and current velocity distribution for the special section with a sudden change in bottom depth are shown in Fig. 6. The temperature distribution is characterized by large horizontal temperature gradients at the thermal bar zone, which indicates a strong mixing there. The thermal bar is, as assumed above, located close to the position of the change in bottom depth. The main part of the shallow region is stably stratified. The inclined isotherms indicate heat advection towards the thermal bar. The deep part of the section is vertically well-mixed with almost depth constant temperatures. The circulation in the section is qualitatively similar to previously shown cases for sections A and B with one circulation cell on each side of the bar, but is more pronounced on the offshore side (mainly due to the enhanced pressure gradient, caused by both horizontal temperature and depth changes, at the position of the rapid increase in bottom depth) than on the onshore side. The maximum horizontal velocities for both the near-shore and convectively mixed region is found close to the bar and is about 1 and 4 cm sec^{-1}, respectively. The geostrophic current velocities are generally smaller than the cross-shore velocities in the near-shore region, but several times higher offshore the thermal bar. The bar zone, as a zone of extensive descending motions, is relatively well defined, with a maximum vertical velocity of approximately 1 mm sec^{-1}.

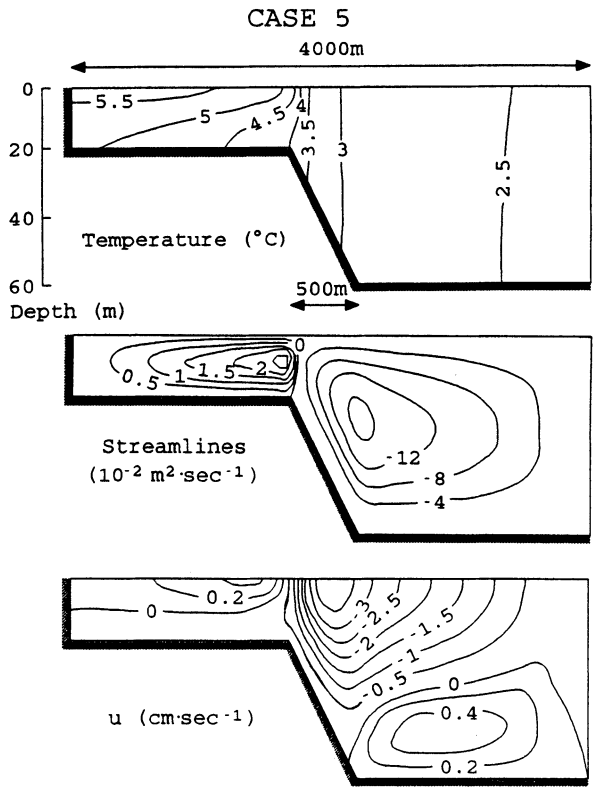

Fig. 6. Obtained temperature distribution, streamfunction, and long-shore velocity distribution for case 5 (section C) when only density-driven currents were considered. Only half of the cross-section is shown as the center is a symmetry line.

Although this case is artificial, it illustrates that the density-induced circulation associated with the thermal bar is of significance at locations with a drastic change in bottom depth. The advection of heat towards the thermal bar may even be larger in reality than as computed here, since the bottom depth normally increases with distance from the shore, which leads to higher mixing and horizontal temperature gradients in the thermal bar zone, and consequently a more pronounced circulation in the bar zone.

Spring Circulation Influenced By Wind

In the previous theoretical calculations, no consideration was taken to the influence of wind on the circulation pattern. In general this is not very realistic. An example of the wind velocities experienced during spring in Lake Ladoga is shown in Fig. 7.

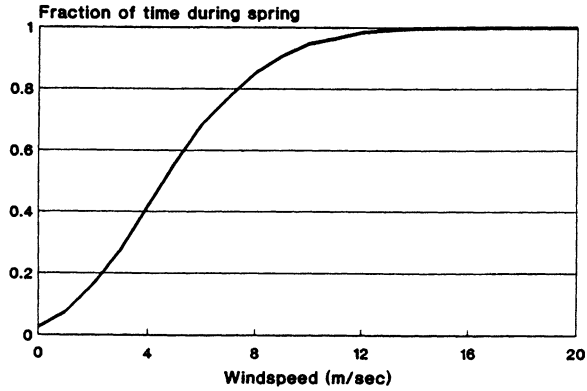

Fig. 7. The accumulated fraction of time *versus* wind velocity during spring in Lake Ladoga. The graph is based on data from a meteorological station at an island in the southern part of Lake Ladoga. The data are from May and June during 5 years (1982, 1983, 1984, 1986, and 1988), where the velocities were measured with 3 hours intervals.

The values are based on 5 years data for May and June. The spring is normally quite calm with only a few occasions of strong wind, which is also the case in Lake Ontario, Csanady (1972).

Preliminary Analysis of the Relative Importance of Wind-driven and Density-induced Currents

The relative importance of wind-driven and density-induced currents in the vicinity of the thermal bar for different wind and horizontal temperature stratification conditions can roughly be estimated by comparing the wind force at the water surface with the pressure force due to the horizontal temperature gradient. The pressure force, directed along the section, on a water column with unit surface area can be expressed as

$$F_P = \int_{-D}^{0} -\frac{\partial p}{\partial y}\, dz \tag{22}$$

For a wind blowing along the section, the wind force at the water surface of the column is (see Eq. 11)

$$F_W = C_D \rho_a W^2 \tag{23}$$

If vertically well-mixed conditions are assumed, *i.e.*, depth isothermal conditions, the density only depends on the distance along the section, y. If also the pressure is assumed hydrostatic, the pressure gradient along the section can be expressed as

$$\frac{\partial p}{\partial y} \approx -\frac{\partial \rho}{\partial y} gz + \rho_m g \frac{\partial h_s}{\partial y} \tag{24}$$

where h_s is the deviation of the water surface from its mean level. The first term on the right-hand side of Eq. (24) expresses the pressure gradient due to the horizontal density (temperature) gradient, while the second term considers the pressure gradient due to the sloping water surface. This second term is related to the continuity requirement for the whole section of the lake, and is therefore of no interest and consequently omitted in the following preliminary analysis. The relative importance of the pressure force due to the horizontal temperature stratification and the wind force can thus be expressed as

$$\frac{F_p}{F_W} = -\frac{(\partial\rho/\partial y)\, g\, D^2}{2C_D\, \rho_a\, W^2} \tag{25}$$

An expression for the horizontal density gradient can be obtained by crudely assuming that the heat entering a water column through the surface in spring remains in the column, and that the vertical mixing is strong enough to create depth-constant temperatures (this is not very realistic for the main part of the region with temperatures above 4°C, but should give reasonable values on the density gradient in the vicinity of the 4°C isotherm). Then, the temperature field can be described by the following expression (Malm and Jönsson 1993)

$$T = T_0 + \frac{Q_s\, t}{\rho_0\, c_p\, D(y)} \tag{26}$$

where T_0 is the initial temperature in the lake when spring heating begins and Q_s as before is the surface heat flux. If the bottom slope is constant, the depth can be expressed as: $D(y) = D_0 + \mu y$, where D_0 is the depth at the shore, and μ is the bottom slope. The horizontal density gradient then becomes (T_0 is assumed to be constant throughout the lake)

$$\frac{\partial\rho}{\partial y} \equiv a\, \rho_m\, \tilde{\mu}(T-T_m)\, \frac{Q_s\, t}{\rho_0 c_p (D_0+\mu y)^2} \tag{27}$$

where the quadratic form of the state equation (Eq. (7)) has been used. Then Eq. (25) becomes

$$\frac{F_P}{F_W} = \frac{a\, g\, \mu\, \rho_m\, Q_s\, t\,(T-T_m)}{2\rho_0 c_p\, C_D \rho_a\, W^2} = \frac{a\, g\, \mu\, \rho_m\, D_T (T-T_m)\,(T-T_0)}{2\, C_D\, \rho_a\, W^2} \tag{28}$$

where D_T is the depth at the position of the T°C isotherm. Thus, the pressure force influence is determined mainly by the bottom slope and the depth. This means that the influence of the density-induced circulation in the vicinity of the thermal bar is greater when the bar is located at larger depths, and when the bottom slope is large. The relative importance of the pressure force, due to the horizontal temperature gra-

Table 4 – The relative importance of the pressure force, due to the horizontal temperature gradient, and the wind force in the vicinity of the thermal bar for section A and section B during conditions with weak, moderate, and strong wind

	Section A	Section B
T_0 (°C)	1	1
T (°C)	5	5
μ	10^{-2}	10^{-3}
Q_s (W m^{-2})	210	210
t (days)	42	22
$\partial\rho/\partial y$ (kg m^{-4})	1.46×10^{-5}	2.78×10^{-6}
	*($\sim1.2\times10^{-5}$)	*($\sim2.7\times10^{-6}$)
F_P/F_W, W = 2 m sec^{-1}	22.6	1.18
F_P/F_W, W = 6 m sec^{-1}	2.5	0.13
F_P/F_W, W = 10 m sec^{-1}	0.9	0.05

* Horizontal density gradients at the 5°C isotherm for sections A and B, based on the results from the hydrodynamic model, and estimated from Fig. 2 (case 2) and Fig.3 (case 4).

dient, and the wind force for section A (slope=10^{-2}) and section B (slope=10^{-3}) during conditions with weak, moderate, and strong wind is given in Table 4. A temperature of 5°C is here chosen to represent the temperature field in the vicinity of the thermal bar (a temperature of 3°C on the other side of the 4°C isotherm will give the same result but with opposite sign). The values of the different constants in Eq. (28) are taken from above.

During conditions with weak winds, the pressure force dominates over the wind force in the steep sloping section, and the density-induced circulation can be expected to be very important. At larger wind speeds (moderate to strong winds) the wind and pressure force, and thus the corresponding currents, are of about the same order of magnitude. In the less sloping section, the wind- and density-driven currents seem to be of equal importance during conditions with weak winds, while the wind-driven circulation dominates when the wind speed increases.

Analysis of the Relative Importance of Wind- and Density-driven Circulation with the Hydrodynamic Model

To get a measure of the relative importance of wind- and density-driven circulation, some simple calculations are made for different scenarios. A dominant density-driven circulation is here defined as consisting of two circulation cells along a cross-section, one on each side of the thermal bar, while the wind-driven circulation is characterized by a single circulation cell that covers the entire section. The initial conditions are the temperature structures and density-driven double-cell circulations for case 2 (section A) and case 4 (section B) shown in Figs. 2 and 3 (section A and B, with constant bottom slopes, are more general than C, with a sudden change in bottom depth, and cases 2 and 4, where vertical heat mixing due to wind was consid-

ered, are more commonly observed types of temperature structures during spring than cases 1 and 3). Wind stresses of different magnitudes and with directions either along or perpendicular to the section are imposed on the water surface. The durations of the imposed wind events are chosen based on the time needed for establishing the wind influence on the circulation. A characteristic time for establishment of such friction-dominated motions was defined by Greenspan and Howard (1963) see also Csanady (1968)

$$t_{\text{setup}} = \frac{D}{\sqrt{fA_v/2}} \tag{29}$$

where t_{setup} is the wind setup time and D is depth. Introducing the following typical values, D=100 m for section A (slope=10^{-2}) and D=50 m for section B (slope=10^{-3}); f=1×10^{-4} sec^{-1}; A_v=1.0×10^{-2}, the wind setup times are 1.64 days (section A) and 0.82 days (section B). As the required period of time for establishment of the wind-induced circulation pattern is longer for stable (smaller exchange coefficients) than for neutral stratification in the near-shore region, the duration of the wind events with low and moderate wind is set to 4 days for section A and 2 days for section B. For events with high wind speeds (≥10 m sec^{-1}), a time characteristic for storm events corresponding to 1 day is used (which is based on the data presented above from Ladoga).

The parameters and initial conditions used in the model calculations for sections A and B are summarized in Table 5.

Table 5 – Parameters used in the numerical calculations for sections A and B of the spring circulation influenced by wind. t_{tot} is the total simulated time from the initial conditions; Δt, Δy, and Δz are the time step, horizontal and vertical grid steps, respectively

Section	A	B
Given initial conditions	Case 2, Fig. 2	Case 4, Fig. 3
Q_s (W m^{-2})	210	210
A_h (m^2 sec^{-1})	0.73	6.25
K_h (m^2 sec^{-1})	0.73	6.25
A_v (m^2 sec^{-1})	$^{1)}1\times10^{-2}(1+10\,R_i)^{-0.5}$, $^{2)}1\times10^{-2}$	$^{1)}1\times10^{-2}(1+10\,R_i)^{-0.5}$, $^{2)}1\times10^{-2}$
K_v (m^2 sec^{-1})	$^{1)}1\times10^{-2}(1+3.33\,R_i)^{-1.5}$, $^{2)}1\times10^{-1}$	$^{1)}1\times10^{-2}(1+3.33\,R_i)^{-1.5}$, $^{2)}1\times10^{-1}$
t_{tot} (days)	4	2
Δt (sec)	1,800	900
Δy (m)	250	1,250
Δz (m)	5	2.5

$^{1)}R_i \geq 0$, $^{2)}R_i < 0$

Table 6 – Relative importance of wind- and density-driven circulation for sections A and B. The analysis is based on the results of calculations of velocity fields for imposed winds of different magnitudes and directions

		Section A (bottom slope = 10^{-2})	Section B (bottom slope = 10^{-3})
Wind along the section	Low wind speeds (1-3 m sec^{-1})	The secondary circulation is characterized by four circulation cells. A zone of convergence with pronounced descending water motions (maximum vertical velocities of the order of 0.5 mm sec^{-1}) is located at the 4°C isotherm. Thus, the thermal bar is still preventing horizontal water exchange and the density-induced circulation is dominating.	The secondary circulation is characterized by a single circulation cell that covers the entire cross-section. The wind-driven circulation is dominating.
	Moderate wind speeds (4-7 m sec^{-1})	A single circulation cell covers the surface layer along the section. Isolated circulation cells (due to the horizontal density gradients) in the bottom layer at the position of the 4°C isotherm, reduces the horizontal water exchange. A transition towards a wind-dominated circulation occurs.	-"-
	High wind speeds (≥8 m sec^{-1})	A single circulation cell covers the entire cross-section (very limited and weak density-induced circulation cells close to the bottom and about the position of the 4°C isotherm are still visible at a wind speed of 8 m sec^{-1}). Wind-driven circulation is dominating.	-"-
Wind perpendicular to the section	Low wind speeds (1-4 m sec^{-1})	The secondary circulation is characterized by three cells (a fourth weak density-driven cell exists close to the bottom at wind speeds of 1-2 m sec^{-1}). The wind-driven circulation dominates over half of the cross-section, while the 4°C isotherm on the other half is a zone of convergence that separates two circulation cells. The thermal bar at this latter half, effectively inhibits horizontal advective volume transport of water and is characterized by strong descending motions (maximum vertical velocities of the order of 3 mm sec^{-1} at a wind speed of 4 m sec^{-1}). Thus, the circulation in the cross-section is partially dominated by wind-driven currents and partially by density-driven currents.	-"-
	Moderate and high wind speeds (≥5 m sec^{-1})	A single circulation cell cover the entire cross-section (at moderate wind speeds, 5-6 m sec^{-1}, a weak density driven circulation cell still exists close to the bottom at one of the 4°C isotherms). Wind-driven circulation is dominating.	-"-

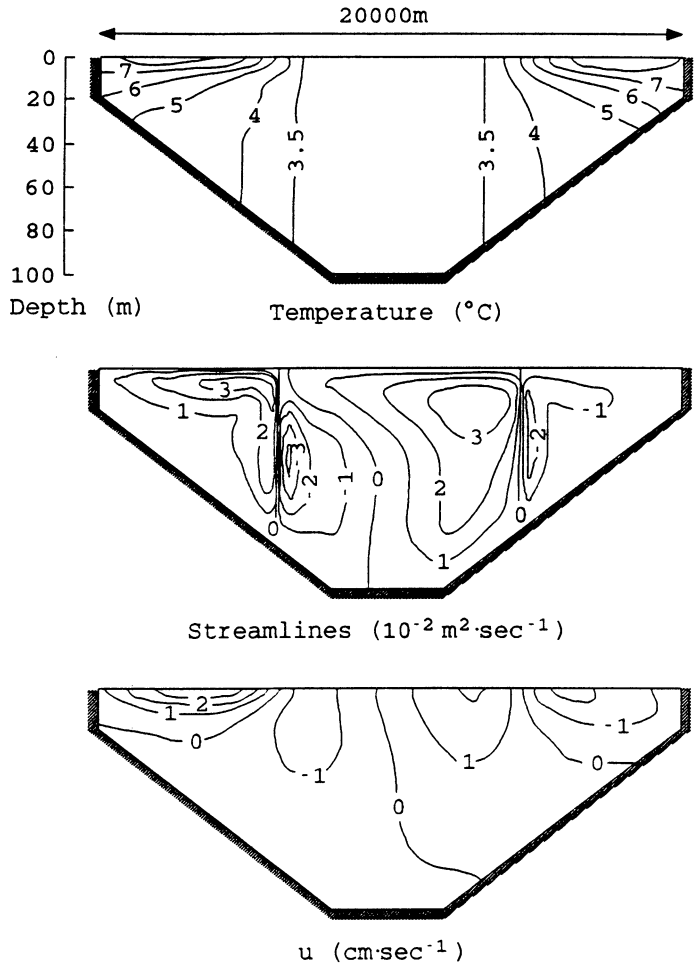

Fig. 8. Temperature distribution, streamfunction, and long-shore velocity distribution for wind- and density-driven currents for section A. The imposed wind speed is 2 m sec^{-1} along the section (from left to right).

The results from the calculations are summarized in Table 6. In Figs. 8 and 9, the calculated velocity and temperature fields for section A (slope ≡ 10^{-2}) are given for occasions with weak and moderate wind speeds when the wind is directed along the section. These velocity distributions show a more or less pronounced influence of the density-driven currents. For low wind speeds (1-3 m sec^{-1}) along the section the density-driven circulation dominates over the wind-driven circulation, with complete circulation cells on each side of the bar. The thermal bar zone effectively inhibits all advective volume transport of water and is characterized by strong descending motions. At moderate wind speeds (4-7 m sec^{-1}) along the section there is a transi-

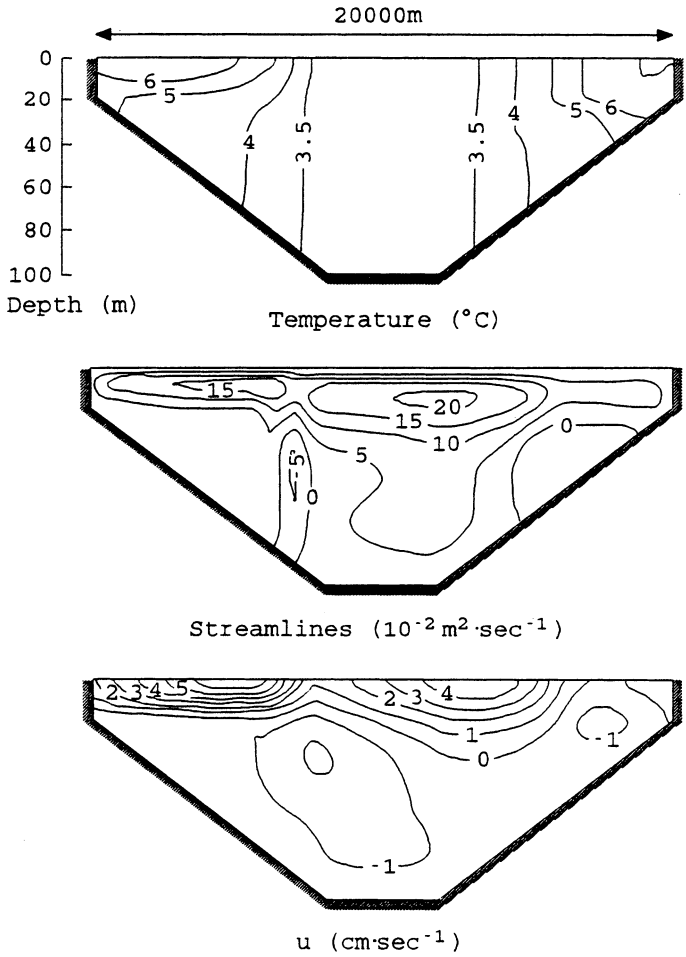

Fig. 9. Temperature distribution, streamfunction, and long-shore velocity distribution for wind- and density-driven currents for section A. The imposed wind speed is 6 m sec^{-1} along the section (from left to right).

tion from a dominating density-driven circulation to a dominating wind-driven circulation. A wind-driven circulation cell covers the upper layer of the cross-section, while two limited density-driven circulation cells are visible in the bottom layer at the vicinity of the 4°C. It can also be noted that the advective volume transport of water is reduced at the thermal bar zone. At high wind speeds (≥8 m sec^{-1}) along the section, the wind-driven circulation covers the whole section, with only a small influence of the density distribution.

If the wind is directed perpendicular to the section (Fig. 10) a somewhat different secondary circulation is obtained. The influence of the thermal bar on the left hand

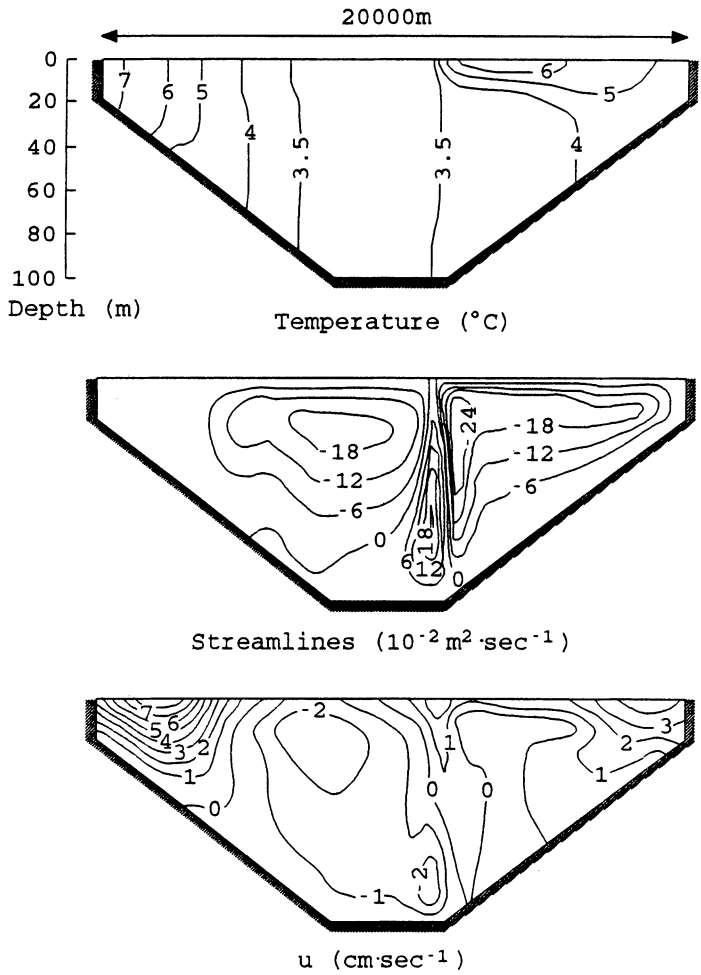

Fig. 10. Temperature distribution, streamfunction, and long-shore velocity distribution for wind- and density-driven currents for section A. The imposed wind speed is 4 m sec^{-1} along the shore line (out from the paper).

side of the section disappears already during low wind speeds, while the circulation and descending motions at the thermal bar on the right hand side become more pronounced. For the situation in Fig. 10, the maximum vertical velocity in the thermal bar zone is about 3 mm sec^{-1}, which is very high. The density-driven circulation in the vicinity of the thermal bar on the right hand side is dominant at low wind speeds (1-4 m sec^{-1}), while a transition towards a dominating wind-driven circulation occurs at moderate wind speeds (5-6 m sec^{-1}).

An interesting detail of the near-shore temperature distribution on the right-hand side in Fig. 10, is the »lens«-shaped thermocline. This peculiar shape of the thermo-

cline was theoretically explained by Csanady (1971) as primarily caused by the inertial adjustment to geostrophic equilibrium, and has been observed at several occasions, *e.g.*, in Lake Ontario (Csanady 1972; 1974).

The influence of the horizontal density gradients in section B (slope = 10^{-3}) is less pronounced, and the wind-driven circulation, characterized by a single circulation cell that covers the whole cross-section, dominates already at very low wind speeds. Thus, it can be concluded that the importance of the density-driven currents during spring in a large temperate lake is strongly dependent on the configuration of the bottom topography.

The results from the force driving analysis of the importance of the wind- and density-driven circulation is in good agreement with the results from the hydrodynamic model. The simpler approach overestimates the importance of the density-driven currents, however. This is because horizontal mixing induced by wind decreases the horizontal density gradients.

The time required to restore a dominating density-induced circulation after an occasion with strong wind is of the order of 1 week for lakes with bottom slopes in the range 10^{-2}-10^{-3}. Thus, it is likely that the current distribution always will be rather complex, with effects of previous and present wind conditions superimposed on the density-driven circulation.

Conclusions

The general density-driven circulation in a large temperate lake is strongly dependent on the bottom topography. The conditions for the density-induced circulation to be of importance, with pronounced descending motions in the thermal bar zone, were shown to be more favorable when the bottom slope is relatively steep. It was also shown that the density-induced currents are of significance in a shallow lake, when the thermal bar is positioned at a location with an abrupt increase in bottom depth.

The model simulations further showed, as an analysis of the driving forces did, that the influence of the density-driven circulation during windy conditions is most significant in lakes with a steep sloping bottom, especially at low and even moderate wind speeds. The thermal bar inhibits horizontal advective volume transport of water at low wind speeds and also have a reducing effect when the wind speed increases. In shallow lakes with flat bottoms, the wind-driven circulation dominates, and the effect of density-induced currents can be expected to be marginal, except at locations with an abrupt change in bottom depth.

Acknowledgements

This work was funded by the Swedish Natural Science Research Council and the Royal Swedish Academy of Sciences. Particular thanks to Professor Lars Bengtsson, Department of Water Resources Engineering, Lund University, for his suggestions and comments in earlier drafts of this manuscript and to Dr. Lennart Jönsson, Department of Water Resources Engineering, and Dr. Arkady Terzhevik, Institute of Limnology, St. Petersburg, Russia, for beneficial discussions.

References

Bennett, J. R. (1971) Thermally driven lake currents during the spring and fall transition periods, Proc. 14th Conf. Great Lakes Res., Intern. Assoc. Great Lakes Res., pp. 535-544.

Bennet, J. R. (1974) On the dynamics of wind-driven lake currents, *J. Phys. Oceno., Vol. 4*, pp. 400-414.

Bowman, M. J., and Okubo, A. (1978) Cabbeling at thermocline fronts, *J. Geophys. Res., Vol. 83*, No. C12, pp. 6173-6178.

Brooks, J., and Lick, W. (1972) Lake currents associated with the thermal bar, *J. Geophys. Res., Vol. 77*, No. 30, pp. 6000-6013.

Carmack, E. C., and Farmer, D. M., (1982) Cooling processes in deep temperate lakes: a review with examples from two lakes in British Columbia, *J. Mar. Res., Vol. 40*, Suppl., pp. 85-111.

Csanady, G. T. (1968) Motions in a model Great Lake due to a suddenly imposed wind, *J. of Geophys. Res., Vol. 73*, No. 20, pp. 6435-6447.

Csanady, G. T. (1971) On the equilibrium shape of the thermocline in the shore zone, *J. Phys. Oceanogr., Vol. 1*, No. 2, pp. 263-270.

Csanady, G. T. (1972) The coastal boundary layer in Lake Ontario. Part 1: The spring regime, *J. Phys. Oceanogr., Vol. 2*, No. 1., pp. 41-53.

Csanady, G. T. (1974) Spring thermocline behavior in Lake Ontario during IFYGL, *J. Phys. Oceanogr., Vol. 4*, No. 3, pp. 425-445.

Elliott, G. T. (1971) A mathematical study of the thermal bar, Proc. 14th Conf. Great Lakes Res., Intern. Assoc. Great Lakes Res., pp. 545-554.

Greenspan, H. P., and Howard, L. N. (1963) On a time-dependent motion of a rotating fluid, *J. of Fluid Mech., Vol. 17*, pp. 385-404.

Harleman, D. R. F., and Stolzenbach, K. D., (1972) Fluid mechanics of heat disposal from power generation, *Annual Rew. of Fluid Mech., Vol. 4*, pp. 7-32.

Henderson-Sellers, B. (1984) *Engineering limnology*, Pitman Publishing Limited, 356 pp.

Huang, J. C. K. (1971) The thermal current in Lake Michigan, *J. Physical Oceanogr., Vol. 1*, No. 2, pp. 105-122.

Huang, J. C. K. (1972) The thermal bar, *Geophys. Fluid Dyn., Vol. 3*, No. 1, pp. 1-25.

Malm, J., and Jönsson, L. (1993) A study of the thermal bar in Lake Ladoga using water surface temperature data from satellite images, *Remote Sensing of the Environment, Vol. 44*, pp. 35-46.

Malm, J., Mironov, D., Terzhevik, A., and Grahn, L. (1991) An investigation of the thermal bar in Lake Ladoga during the spring 1991, Department of Water Resources Engineering, Lund University, Report No. 3150, Lund, Sweden, 92 pp.

Malm, J., Mironov, D., Terzhevik, A., and Grahn, L. (1992) A field study of the thermal bar in Lake Ladoga – spring 1992 – Department of Water Resources Engineering, Lund University, Report 3162, Lund, Sweden, 78 pp.

Malm, J., Mironov, D., Terzhevik, A., and Grahn, L. (1993) Field investigation of the thermal bar in Lake Ladoga, spring 1991, *Nordic Hydrology, Vol. 24*, pp. 339-358.

Malm, J., Mironov, D., Terzhevik, A., and Jönsson, L. (1994) Investigation of the spring thermal regime in Lake Ladoga using field and satellite data, *Limnology and Oceanography, Vol. 39(6)*, pp. 1333-1348.

Malm, J., and Zilitinkevich, S. S. (1994) Temperature distribution and current system in a convectively mixed lake. Paper accepted for publication in *Boundary Layer Meteorology*.

Munk, W. H., and Anderson, E. R. (1948) Notes on the theory of the thermocline, *J. of Marine Research, Vol. 1*.

Patankar, S. V. (1980) *Numerical heat transfer and fluid flow*, Hemisphere Publishing Corporation, McGraw-Hill Book Company, 197 pp.

Petrova, N. A., and Terzhevik, A., eds. (1992) *Lake Ladoga – ecosystem state criteria*, Nauka Publishing House, St. Petersburg, 325 pp. (in Russian).

Rodgers, G. K. (1965) The thermal bar in the Laurentian Great Lakes. Proc. 8th Conf. Great Lakes Res., Univ. Michigan, Great Lakes Res. Div., Publ. 13, pp. 358-363.

Rodgers, G. K. (1966) The thermal bar in Lake Ontario, spring 1965 and winter 1965-66, Proc. 9th Conf. Great Lakes Res., Univ. Michigan, Great Lakes Res. Div., Publ. 15, pp. 369-374.

Rodgers, G. K. (1968) Heat advection within Lake Ontario in spring and surface water transparency associated with the thermal bar, Proc. 11th Conf. Great Lakes Res., Intern. Assoc. Great Lakes Res., 942-950.

Rodgers, G. K., and Sato, G. K. (1970) Factors affecting the progress of the thermal bar of spring in Lake Ontario, Proc. 13th Conf. Great Lakes Res., Internat. Assoc. Great Lakes Res., pp. 942-950.

Rodgers, G. K. (1971) Field investigation on the thermal bar in Lake Ontario: precision temperature measurements. Proc. 14th Conf. Great Lakes Res., Intern. Assoc. Great Lakes Res., pp. 618-624.

Rodi, W. (1980) Turbulence models and their application in hydraulics. State-of-the-art paper, presented by the IAHR-Section on Fundamentals of Division II: Experimental and Mathematical Fluid Dynamics.

Scavia, D., and Bennett, J. R. (1980) Spring transition period in Lake Ontario – a numerical study of the causes of the large biological and chemical gradients, *Can. J. Fish. Aquat. Sci., Vol. 37*, pp. 823-833.

Spalding, D. B. (1992) *A guide to the phoenics input language*, Concentration, Heat and Momentum Limited, London.

Svensson, U. (1978) A mathematical model of the seasonal thermocline, Department of Water Resources Engineering, Lund University, Report No. 1002, Lund, Sweden.

Tikhomirov, A. I. (1959) About the thermal bar in Yakimvarski Bay of Lake Ladoga, *Proceedings of the All-Union Geographic Society, Vol. 91*, No. 5, pp. 424-438 (in Russian).

Tikhomirov, A. I. (1963) The thermal bar of Lake Ladoga, *Soviet Hydrology, Selected Papers, Am. Geophys. Union Translation, Vol. 95*, No. 2, pp. 134-142.

Zilitinkevich, S. S. (1970) *Dynamics of the atmospheric boundary layer*, Gidrometeoizdat Press, Leningrad, 292 pp. (in Russian).

Zilitinkevich, S. S., Kreiman, K. D., and Terzhevik, A.Yu. (1992) The thermal bar, *J. Fluid Mech.*, No. 236, pp. 27-42.

First received: 10 November, 1994
Revised version received: 5 April, 1995
Accepted: 25 April, 1995

Address:
Department of Water Resources Enginerring,
Lund Inst. of Tech/Lund University,
Box 118,
S-221 00 Lund,
Sweden.